2015

Comparison of experimental respiratory tularemia in three nonhuman primate species

Audrey R. Glynn
Center for Aerobiological Sciences, U.S. Army Medical Research Institute of Infectious Diseases, Fort Detrick, Frederick, MD

Derron A. Alves
Pathology Division, U.S. Army Medical Research Institute of Infectious Diseases, Fort Detrick, Frederick, MD

Ondraya Frick
Center for Aerobiological Sciences, U.S. Army Medical Research Institute of Infectious Diseases, Fort Detrick, Frederick, MD

Rebecca Erwin-Cohen
Center for Aerobiological Sciences, U.S. Army Medical Research Institute of Infectious Diseases, Fort Detrick, Frederick, MD

Aimee Porter
Center for Aerobiological Sciences, U.S. Army Medical Research Institute of Infectious Diseases, Fort Detrick, Frederick, MD

See next page for additional authors

Authors
Audrey R. Glynn, Derron A. Alves, Ondraya Frick, Rebecca Erwin-Cohen, Aimee Porter, Sarah Norris, David Waag, and Aysegul Nalca

Comparative Immunology, Microbiology and Infectious Diseases 39 (2015) 13–24

Contents lists available at ScienceDirect

Comparative Immunology, Microbiology and Infectious Diseases

journal homepage: www.elsevier.com/locate/cimid

Comparison of experimental respiratory tularemia in three nonhuman primate species

Audrey R. Glynn[a,1], Derron A. Alves[b,2], Ondraya Frick[a], Rebecca Erwin-Cohen[a], Aimee Porter[a], Sarah Norris[c], David Waag[d], Aysegul Nalca[a,*]

[a] *Center for Aerobiological Sciences, U.S. Army Medical Research Institute of Infectious Diseases (USAMRIID), Fort Detrick, Frederick, MD 21702, USA*
[b] *Pathology Division, U.S. Army Medical Research Institute of Infectious Diseases (USAMRIID), Fort Detrick, Frederick, MD 21702, USA*
[c] *Biostatistics Division, U.S. Army Medical Research Institute of Infectious Diseases (USAMRIID), Fort Detrick, Frederick, MD 21702, USA*
[d] *Bacteriology Division of U.S. Army Medical Research Institute of Infectious Diseases (USAMRIID), Fort Detrick, Frederick, MD 21702, USA*

ARTICLE INFO

Article history:
Received 12 August 2014
Received in revised form 16 January 2015
Accepted 28 January 2015

Keywords:
Francisella tularensis
Tularemia
Aerosol
Inhalation
Nonhuman primate
Animal model

ABSTRACT

Tularemia is a zoonotic disease caused by *Francisella tularensis*, which is transmitted to humans most commonly by contact with infected animals, tick bites, or inhalation of aerosolized bacteria. *F. tularensis* is highly infectious via the aerosol route; inhalation of as few as 10–50 organisms can cause pneumonic tularemia. Left untreated, the pneumonic form has more than >30% case-fatality rate but with early antibiotic intervention can be reduced to 3%. This study compared tularemia disease progression across three species of nonhuman primates [African green monkey (AGM), cynomolgus macaque (CM), and rhesus macaque (RM)] following aerosolized *F. tularensis* Schu S4 exposure. Groups of the animals exposed to various challenge doses were observed for clinical signs of infection and blood samples were analyzed to characterize the disease pathogenesis. Whereas the AGMs and CMs succumbed to disease following challenge doses of 40 and 32 colony forming units (CFU), respectively, the RM lethal dose was 276,667 CFU. Following all challenge doses that caused disease, the NHPs experienced weight loss, bacteremia, fever as early as 4 days post exposure, and tissue burden. Necrotizing-to-pyogranulomatous lesions were observed most commonly in the lung, lymph nodes, spleen, and bone marrow. Overall, the CM model consistently manifested pathological responses similar to those resulting from inhalation of *F. tularensis* in humans and thereby most closely emulates human tularemia disease. The RM model displayed a higher tolerance to infection and survived exposures of up to 15,593 CFU of aerosolized *F. tularensis*.

Published by Elsevier Ltd.

1. Introduction

The etiological agent of tularemia, *Francisella tularensis*, is a highly infectious and virulent bacterial pathogen known to persist in the environment, infect humans by multiple modalities, including aerosol, and cause high morbidity/mortality by extremely low infectious dose (<10 colony forming units [CFU]) [1]. Frequently included in the

* Corresponding author at: United States Army Medical Institute of Infectious Diseases, 1425 Porter Street, Frederick, MD 21702, USA. Tel.: +1 301 619 8495; fax: +1 301 619 0347.
E-mail address: aysegul.nalca@us.army.mil (A. Nalca).
[1] Present address: Strategic Analysis, Inc., Arlington, VA, USA.
[2] Present address: Defense Health Agency Veterinary Services (DHA VS), Defense Health Headquarters, USA.

http://dx.doi.org/10.1016/j.cimid.2015.01.003
0147-9571/Published by Elsevier Ltd.

former Soviet Union and various international bioweapons programs throughout history, the bacterium's high virulence and capacity to be weaponized led the United States (US) Centers for Disease Control and Prevention (CDC) and the National Institute of Allergy and Infectious Disease (NIAID) to classify it as a Category A biothreat select agent [2–5]. Given the significant potential for aerosolized *F. tularensis* as a bioterrorism agent, the need for a well-characterized animal model of aerosol transmission is clear.

In 2002, the US Food and Drug Administration (FDA) implemented the *Animal Rule* for approval of vaccines and therapeutics when human efficacy studies are not ethical or feasible (21 CFR 314.610 and 21 CFR 601.91). This regulation has driven the development of well-characterized animal models designed to resemble human disease to enable high-confidence testing of medical countermeasures against biothreat agents.

Mice, rats, rabbits, and nonhuman primates (NHPs) all have been used to model the efficacy of therapeutics and vaccines against *F. tularensis* [6]. Although studies in literature indicate that the NHP model resembles tularemia disease in humans better than other models, published data lacks critical findings regarding well-characterized animal models for *Animal Rule* applications, such as clinical signs, clinical pathology, and gross and microscopic pathology [7].

In this series of experiments, a side-by-side disease progression study designed to identify the disease markers resulting from highly virulent *F. tularensis* Schu S4 aerosol exposure of three NHP species, African green monkeys (AGM), cynomolgus macaques (CM), and rhesus macaques (RM) was conducted for the first time. The resulting data contain critical evidence supporting the selection and development of an inhalational tularemia animal model that adequately mimics inhalational tularemia in humans.

2. Materials and methods

2.1. Animals

Healthy, adult AGM (*Chlorocebus aethiops*) ($n = 5$), CM (*Macaca fascicularis*) ($n = 6$), and RM (*Macaca mulatta*) ($n = 5$) of both sexes were obtained from the US Army Medical Research Institute of Infectious Diseases (USAMRIID) approved commercial vendors. Animals were in good physical condition and were free of clinical signs of any infection. Research was conducted under an IACUC approved protocol in compliance with the Animal Welfare Act, PHS Policy, and other Federal statutes and regulations relating to animals and experiments involving animals. The facility where this research was conducted is accredited by the Association for Assessment and Accreditation of Laboratory Animal Care, International and adheres to principles stated in the Guide for the Care and Use of Laboratory Animals, National Research Council, 2011.

2.2. Challenge agent

The *F. tularensis* Schu S4 strain was provided by NIAID. A flask of Mueller Hinton II (MHII) liquid medium + 2% isovitalex enrichment was inoculated with a *F. tularensis* Schu S4 seed stock. The culture was incubated for 23 h at 37 °C with shaking at a speed of 200 rpm. Following incubation, the culture was measured for OD (660 nm) and the concentration of microorganisms was determined according to a predetermined mathematical relationship between concentration and OD. The microorganisms were diluted in MHII liquid media to the desired nebulizer starting concentrations.

2.3. Aerosol exposure

Each NHP was anesthetized by intramuscular (IM) injection of tiletamine/zolazepam (6 mg/kg) and then subjected to whole body plethysmography (Buxco Research Systems, Wilmington, NC) for determination of the respiratory minute volume (MV) as previously described [8]. Subsequently, each NHP was exposed to *F. tularensis* Schu S4 in a head-only chamber contained within a class III biological safety cabinet located within a biosafety level 3 (BSL-3) suite. The Automated Bioaerosol Exposure System (ABES) served as the control platform for the aerosol exposures [9]. Aerosol particles were generated by a three-jet collison nebulizer (BGI, Inc., Waltham, MA). An all glass impinger (AGI) was used to collect integrated air samples for each aerosol run.

After exposure, several dilutions prepared from each AGI sample were used to inoculate Modified Thayer Martin (MTM) agar plates for analysis. The inhaled *F. tularensis* Schu S4 dose was calculated for each NHP based on the bacterial growth that resulted from AGI samples and dilutions and from the minute volume (MV) measurement.

2.4. Telemetry

A radiotelemetry device TA10TA-D70 (Data Sciences International [DSI], St. Paul, MN) was used to monitor body temperature following surgical implantation into each NHP at least 14 days before exposure. Body temperatures were recorded every 15 min by the DataQuest A.R.T.4.1 system (DSI). Pre-exposure baseline temperature data were used to calculate a baseline by averaging the recorded 15 min temperature intervals for at least 9.5 consecutive hours on day −1. Fever was defined as an elevation of body temperature >1.5 °C above baseline values for at least 6 consecutive hours.

2.5. Clinical observation

NHPs were observed and scored at least twice a day following aerosol exposure. The scoring parameters were; activity (1: normal, 2: active, 3; less active, 4: sluggish, 5: inactive), behavior (1: normal, 2: antisocial, 3: depressed, 4: hunched, 5: ignoring everything), stimuli response (1: normal, 2: entering room, 3: approaching cage, 4: rattling cage, 5: pinching), breathing (1: normal, 2: rapid, 3: abdominal, 4: agonal, 5: rales). The early endpoint criteria monitored for humane euthanasia, indicative of very poor health status, were cumulative clinical scores of 16–20 (maximum score), and/or sudden drop of >3 °C from baseline body temperature.

2.6. Complete blood counts (CBCs)

Beginning one to two days before exposure, and every other day between days 2–28 PE, blood samples were collected from the femoral vein of NHPs anesthetized with tiletamine/zolazepam (3 mg/kg). Beckman Coulter hematology analyzers (Brea, CA) were used to analyze CBCs according to the manufacturer's instructions.

2.7. Quantitative bacteremia by real time quantitative PCR assay

Bacterial DNA was extracted from 100 μl samples of blood using Qiagen (Valencia, CA) QIAamp DNA blood kit according to the manufacturer's instructions. Real-time qPCR was performed with the LightCycler (Roche, Indianapolis, IN) using a *F. tularensis* (*tul4*) gene-specific assay [10]. The positive extraction control samples (PEC) was generated by spiking defined amounts of *F. tularensis* culture into uninfected blood samples, and extracting the DNA.

2.8. Cytokine analysis

Plasma cytokine detection was performed using the BIORAD Bio-Plex™ 200 Multiplex Array System (Bio-Rad Laboratories, Hercules, CA) and Bio-Plex™ Pro Human Cytokine 17-Plex Assay kit (Bio-Rad Laboratories, Hercules, CA) per the manufacturer's instructions to evaluate the levels of IL-1β, IL-2, IL-4, IL-5, IL-6, IL-7, IL-8, IL-10, IL-12, IL-13, IL-17, G-CSF, GM-CSF, IFN-γ, MCP-1 (MCAF), MIP-1β, and TNF-α.

2.9. Necropsy and macroscopic pathology

Necropsies were performed in BSL-3 on animals humanely euthanized when moribund or at the conclusion of the study by (or under the direct supervision of) a veterinary pathologist board certified by the American College of Veterinary Pathologists. Each complete set of necropsied tissues included lymph nodes (mediastinal/tracheobronchial, mandibular, axillary, inguinal, and mesenteric), tongue, tonsil, heart, thymus, lung, spleen, liver, adrenal gland, kidney, urinary bladder, testes or ovary, prostate gland or uterus, stomach, duodenum (with pylorus), pancreas, jejunum, ileum, ileocecal junction, colon, sciatic nerve, skeletal muscle, bone marrow, eyes, brain, pituitary gland, and haired skin. For histology and immunohistochemistry analyses, tissue samples collected from each animal were immersion-fixed in 10% neutral-buffered formalin for a minimum of 21 days. Portions of lung, kidney, spleen, liver, lymph nodes, adrenal gland, heart, and brain were submitted for bacterial culture at the time of postmortem examination.

2.10. Histology and immunohistochemistry

For light microscopy, all formalin-fixed tissues from all animals were processed, embedded in paraffin wax, sliced into 5–6 μm section using a rotary microtome, mounted on glass slides, and stained with hematoxylin and eosin (HE). Immunohistochemical staining *for F. tularensis* was performed on all tissues selected from 7 animals: 2 AGMs, 2 CMs, and 3 RMs. Serial sections of these tissues were cut and stained for *F. tularensis* lipopolysaccharide (LPS) (Meridian Life Science, Inc., Cincinnati, OH) and visualized using a mouse monoclonal antibody to *F. tularensis* LPS (Meridian Life Science, Inc., Cincinnati, OH) at a (USAMRIID immuno #927) and an immunoperoxidase assay system (EnVision System, DAKO Corp., Carpinteria, CA). Normal lung tissue was used as a negative control and lung from a known *F. tularensis* Schu S4-infected AGM was used as a positive control. Normal mouse IgG was used as the negative serum control. For the immunohistochemistry study, the unstained tissue sections were deparaffinized, blocked using methanol–hydrogen peroxide, pretreated with proteinase K, incubated with serum-free protein block (DAKO) plus 5% normal goat serum followed by the monoclonal antibody at a dilution of 1:1200, and finally exposed to the EnVision horseradish peroxidase labeled polymer. All sections were exposed to 3,3′-diaminobenzidine (DAB) permanent chromogen, counter-stained with hematoxylin, and covered with Permount (Thermo Fisher Scientific, Waltham, MA).

2.11. Statistical analysis

NHP temperatures were collected daily to assess changes over time. Repeated measures analysis of variance (RM-ANOVA) was completed, however, only for time points falling within the day −1 to day 6 post-exposure (PE) timeframe. Comparisons of individual time points were completed for all groups through day 14 PE. Analyses of variance (ANOVA) were used to compare body weights at each individual time point (with post hoc Tukey's tests for pairwise comparisons) for days 0, 2, 4, 6, 8, and 10 PE. Beyond day 10 PE, the numbers of samples were insufficient to perform ANOVA.

For CBCs, ANOVA was used to test for group differences at each time point, with post hoc Tukey's tests for specific pairwise comparisons at −2, 2, 4, and 6 (between all NHP groups) and 8, 10, 12, and 14 days PE (for comparison between CM and RM groups). Beyond day 14 PE, sample sizes were insufficient for comparison. For blood and tissue bacterial loads Kruskal–Wallis tests were conducted with Wilcoxon–Mann–Whitney tests for pairwise comparison. All analyses were conducted using SAS Version 9.3.

3. Results

3.1. Exposure doses and outcome

In this study, three species of NHPs were aerosol challenged with varied doses of *F. tularensis* Schu S4 (Table 1). A target dose of 100 CFU *F. tularensis* was sufficient to cause the development of lethal disease in two of the three species (AGM and CM). The calculated inhaled doses are listed in Table 1.

Within 2–5 days PE to target doses of 100 CFU or higher, all NHPs displayed increased body temperature, decreased appetite, decreased activity, and other signs of clinical disease. Upon low-dose challenges of 11 and 20 CFU, the AGMs

Table 1
Exposure dose, onset of fever and time to death in individual NHPs.

Animal ID	Target dose (CFU)	Inhaled dose (CFU)	Average day of fever onset[a]	Time of death (Days)	Manner of death
AGM 1	10	11	No fever	NA	Survived
AGM 2	100	40	4	14	Euthanized
AGM 3	100	216	4	8	Found dead
AGM 4	1,000	271	3	6	Euthanized
AGM 5	10,000	10,908	3	6	Euthanized
CM 1	10	20	No fever	NA	Survived
CM 2	100	32	4	22	Euthanized
CM 3	100	186	NA[b]	10	Found dead
CM 4	1,000	332	4	10	Euthanized
CM 5	1,000	801	3	9	Euthanized
CM 6	10,000	11,298	2	6	Euthanized
RM 1	1,000	377	3	NA	Survived
RM 2	3,000	2,693	2	NA	Survived
RM 3	10,000	11,211	3	NA	Survived
RM 4	10,000	15,593	3	NA	Survived
RM 5	100,000	276,667	3	6	Euthanized

[a] Fever defined as an elevation of body temperature >1.5 °C over baseline values, as established on study day −1, for at least 6 consecutive hours for each individual.
[b] Telemetry for this animal was failed, therefore data was not available.
NA: Not applicable.

and CMs, respectively, showed no signs of illness, however both of these species met euthanasia criteria after higher challenge doses (Table 1). The RMs, however, survived challenge doses as high as 15,593 CFU, but succumbed to 276,667 CFU. For AGMs and CMs, death occurred 11 or 16 days PE to 40 CFU (AGM 2) or 216 CFU (AGM 3) and 32 CFU (CM 2) or 186 CFU (CM 3), respectively. The shortest time-to-death occurred 6 days PE following exposure of the AGM with 10, 908 CFU (AGM 5), CM with 11,298 CFU (CM 6), and RM with 276,667 CFU (RM 5).

3.2. Body temperature and weight change

In the AGMs and CMs, fever onset occurred 2–4 days PE depending on the dose level (Table 1); all AGMs and CMs that developed fever eventually met euthanasia criteria. After most of the *F. tularensis* exposure doses used in this study, the RM species developed fever that remained for the duration of the animal's illness (Fig. 1A). RMs exposed to non-lethal doses maintained fever for the longest duration compared to the other species, about 24 days. Within 4 days of challenge, all NHPs (except for AGMs and CMs exposed to the lowest doses) displayed a 1.5 °C elevation in body temperature. RM-ANOVA of temperature from days −1 and through 6 PE indicated that, there were significant overall differences in temperature between groups ($P < 0.0001$), and over time ($P < 0.0001$), but not in the interactive effect of group by time ($P = 0.9118$), supporting the observation of nearly parallel temperature changes between groups over that time period (Fig. 1A). Pairwise group comparisons revealed statistical differences in body temperatures between the RM and either the AGM ($P < 0.0001$) or the CM ($P = 0.0009$). The RMs exhibited significantly higher fever response than AGMs or CMs.

All challenged NHPs, except for the surviving AGM and CM, exhibited disease-related weight loss. The mean weight loss for the RMs was 10% of body weight; whereas the mean weight loss was about 5% for AGMs and CMs (Fig. 1B). The three RMs (RM 3–5) challenged with the highest doses decreased in weight throughout the study period, whereas the two lower dosed RMs (RM 1 and RM 2) lost weight initially, but gained weight with recovery after day 24 PE. Significant differences in daily body weights were not observed among the three species of NHPs at any time point.

3.3. Complete blood counts (CBCs)

The CBCs shifted differentially from baseline for all three NHP species throughout disease progression. Significant increases or decreases were determined for individual NHPs based on baseline values obtained prior to exposure. Overall, white blood cells (WBCs) increased early in disease for all NHPs (Fig. 2A). Whereas WBC levels remained elevated in RMs, the WBC changes in AGMs and CMs were insignificant aside from peaks observed on days 12 and 14 PE. All NHP species exhibited increased granulocyte levels until 6 days PE (Fig. 2B). Whereas RM granulocyte levels remained elevated, AGM and CM granulocyte levels returned to normal about 6 days PE. Similarly, lymphocyte levels increased in RMs around day 10 PE but dropped early in AGMs and CMs (Fig. 1C). With regard to monocyte levels, AGM levels peaked beginning on day 6, while CM and RM levels maintained normal levels (Fig. 1D). For all non-surviving NHPs, platelet counts decreased steadily after exposure (data not shown).

3.4. Cytokine profiles

Serially collected plasma samples were assayed for several cytokines. Prominent fluctuations were observed in IL-6, IL-8, granulocyte-colony stimulating factor (G-CSF),

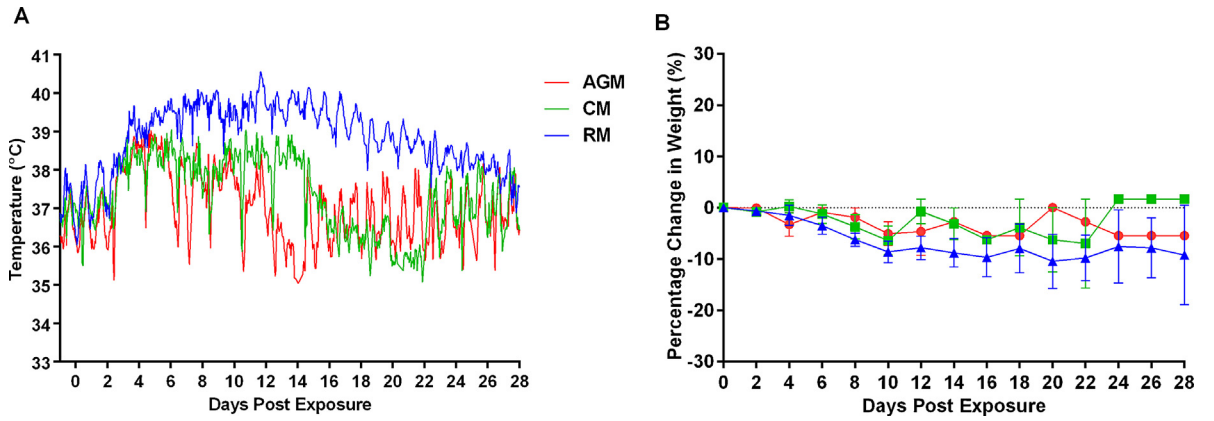

Fig. 1. (A) Mean body temperature variation over time in three NHP species and (B) percentage changes in body weights of CM, AGM, and RM that had been exposed to various doses of aerosolized *F. tularensis*.

IFN-γ, monocyte chemoattractant protein-1 (MCP-1), and MCP-1β profiles. Table 2 compares cytokine profiles in three NHP species exposed to target dose of 1,000 CFU. Similar trends were observed for other challenge doses.

The CMs and AGMs exhibited steady increases in IL-6 levels, whereas the RM IL-6 levels peaked on day 6 PE and decreased thereafter. Just prior to euthanasia, IL-6 in the single RM that was euthanized on day 6 PE elevated 600-fold above baseline (data not shown). All three NHP species showed uniform increases in IL-8 levels just prior to euthanasia. Increased levels of G-CSF and IFN-γ were observed in AGMs and CMs but not in the RMs. Likewise, elevations in MCP-1 and MCP-1β were much greater in AGMs and CMs than in RMs. No significant changes or

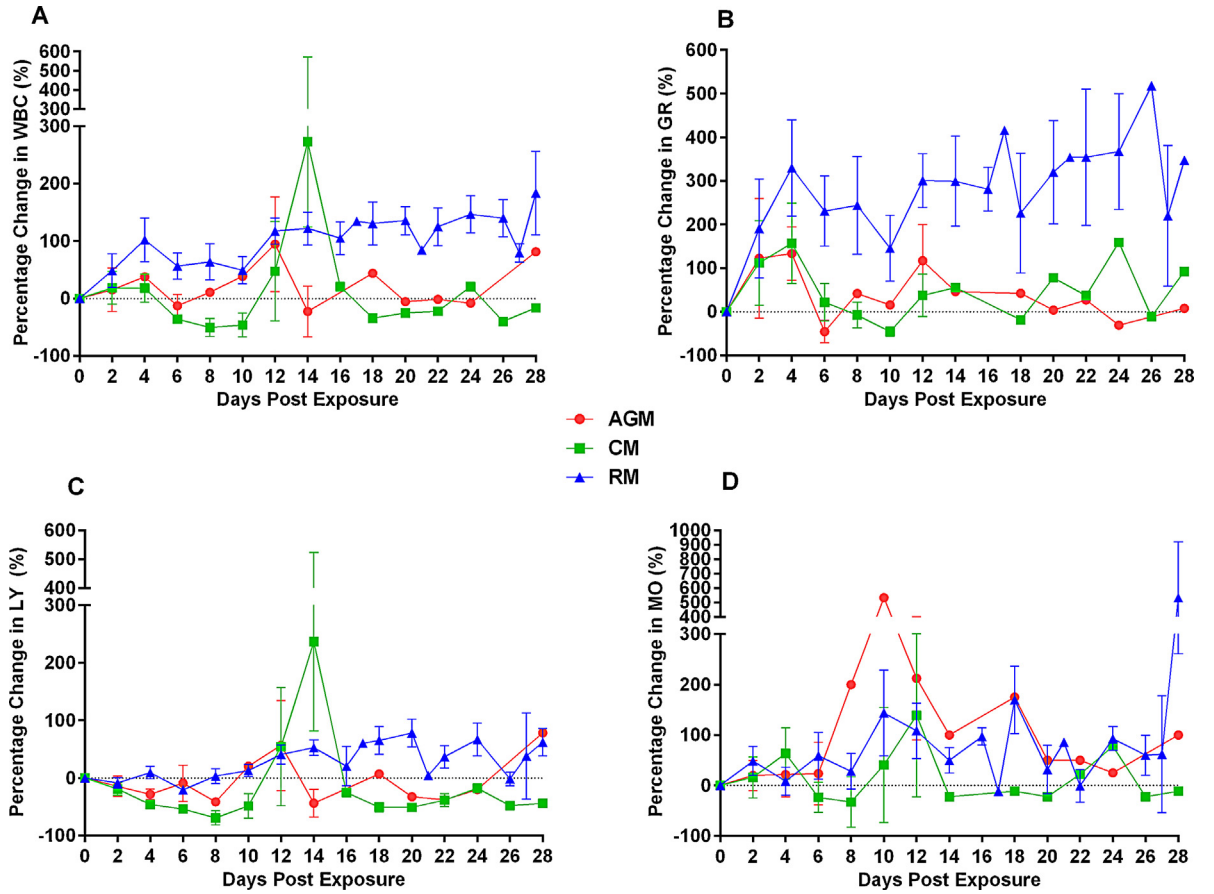

Fig. 2. Percentage changes in (A) white blood cell count (WBC), (B) granulocytes (GR), (C) lymphocytes (LY), and (D) monocytes (MO) over time in CM, AGM, and RM exposed to various doses of aerosolized *F. tularensis*.

Table 2
Comparison of serum cytokine levels (pg/ml) in 3 NHP species exposed to a target dose of 10,000 CFU aerosolized *F. tularensis*.

Cytokines	IL-6			IL-8			G-CSF			IFN-γ			MCP-1			MCP-1β		
Days post exposure	AGM5	CM6	RM3	AGM5	CM6	RM3	AGM5	CM6	RM3	AGM5	CM6	RM3	AGM5	CM6	RM3	AGM5	CM6	RM3
−2	OOR<	OOR<	OOR<	OOR<	12	55	OOR<	OOR<	OOR<	OOR<	OOR<	OOR<	58	18	15	24	51	51
2	13	10	1	OOR<	22	29	4	12	2	OOR<	OOR<	OOR<	63	63	35	24	51	49
4	827	405	53	OOR<	46	15	412	46	1	46	OOR<	OOR<	1111	142	42	365	91	93
6	OOR>	4352	158	2282	783	101	2703	535	9	723	57	OOR<	34,715	1968	56	3371	397	71
8			15			131			OOR<			4			20			13
10			35			91			OOR<			4			20			23
12			10			203			OOR<			13			17			15

OOR<: Out of range below, OOR>: Out of range above.
Measurement unit: pg/ml.

patterns were observed for other cytokines tested (data not shown).

3.5. Bacteremia—blood

Whole blood samples were collected every other day PE and were analyzed for bacterial load by PCR (Fig. 3). The RM blood samples consistently yielded low genome numbers (Fig. 3C). Whereas AGMs and CMs exposed to fatal doses displayed higher bacterial loads detectable as early as days 4 PE (Fig. 3A and B). No differences in bacteremia were evident in pairwise comparison among the NHP groups between days 1 and 10.

3.6. Bacteremia—tissues

At the conclusion of the study, tissue samples were harvested from euthanized NHPs, processed to determine tissue bacterial burden by PCR (Fig. 4). The highest bacterial loads were observed in the lungs and mandibular lymph nodes of AGMs (Fig. 3A). In CMs the brain, lung and spleen contained the greatest numbers of bacteria; and all tissues

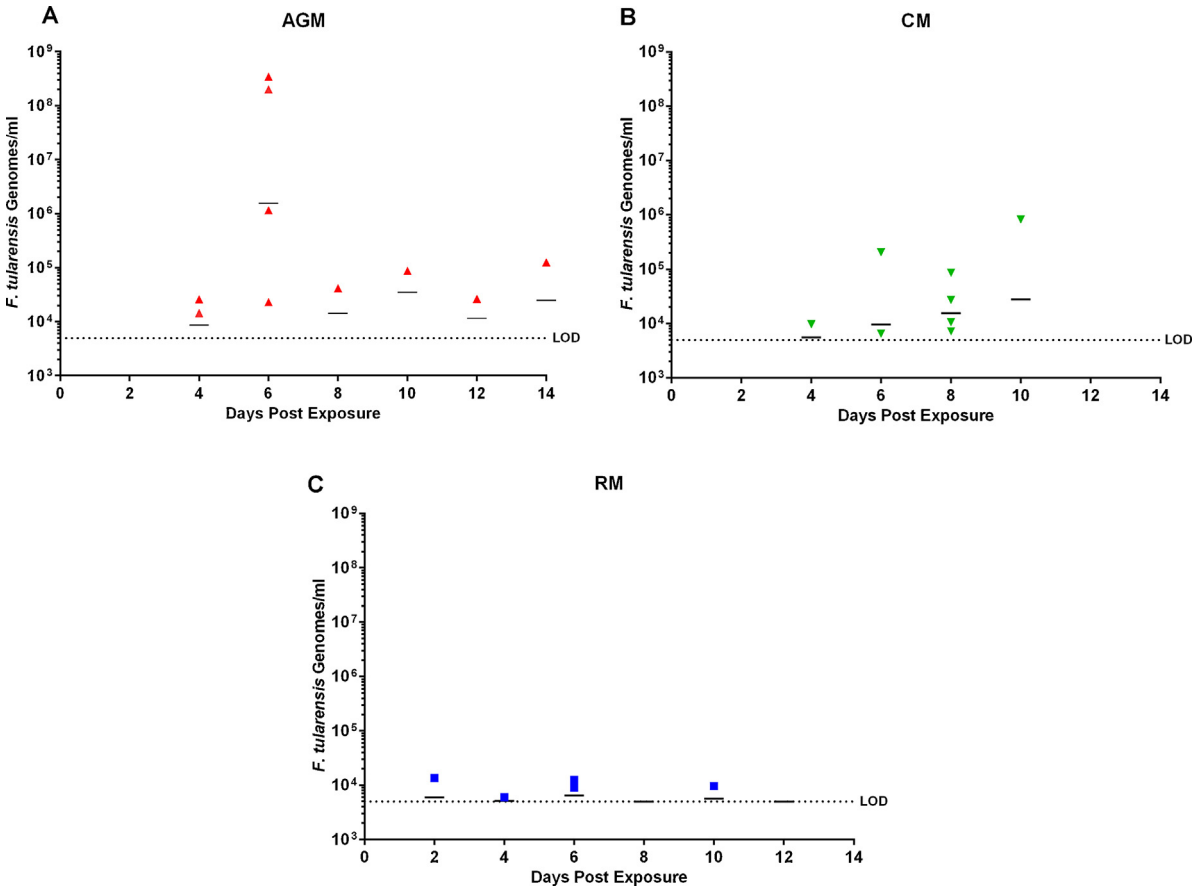

Fig. 3. Bacterial load (genomes/ml) in whole blood of (A) AGM, (B) CM, and (C) RM. Limit of detection (LOD): 5000 genome/ml.

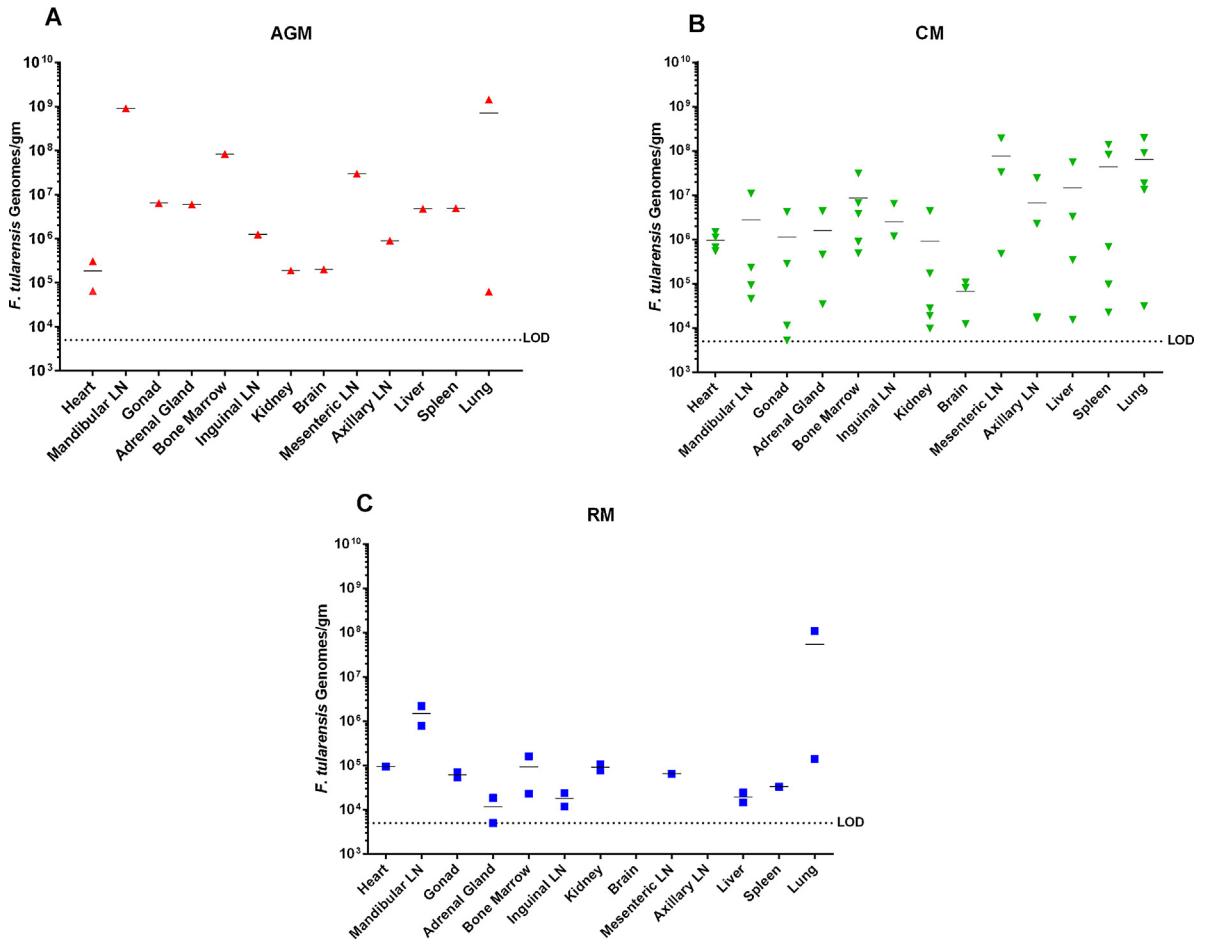

Fig. 4. Bacterial burden (genome/gr) in select tissues obtained from euthanized (A) AGM, (B) CM, and (C) RM exposed to various doses of aerosolized *F. tularensis*. Limit of detection (LOD): 5000 genome/g.

obtained from CMs exposed to fatal doses harbored significant tissue bacterial burden (Fig. 4B). The tissue bacterial burdens in RMs were much lower than in AGMs and CMs with the exception of the lungs (Fig. 4C).

3.7. Pathology

Most of the aerosolized *F. tularensis* challenge doses in this study led to the development of lesions that varied in distribution and severity and affected multiple body systems. Here we describe the pathologic changes observed in the respiratory and hematopoietic systems, which were clearly targets of infection following aerosol administration of *F. tularensis* at any dose.

3.7.1. Necropsy findings

Regardless of the NHP species, dose received, or the time-to-death, the most common macroscopic pathologic changes occurred in the lung, mediastinal and tracheobronchial lymph nodes, and spleen (Fig. 5 and Table 3). Compared to normal lungs (Fig. 5A), diseased lung lobes frequently were enlarged and failed to collapse (Fig. 5C–E). Pulmonary congestion, hemorrhage, and edema with fibrinous pleuritis were evident in the AGM and CM subjects (Fig. 5C–E), whereas fibrous tags between lung lobes and attaching to the thoracic wall were common in RMs that survived the experimental infection. As early as 6 days after challenge, randomly scattered, well-circumscribed-to-coalescing, subacute abscesses and pyogranulomas ranging in size from 6 mm to 2 cm in diameter effaced the pulmonary architecture of the inferior lung lobes but were also distributed randomly in other lobes. The large acute lesions usually were suppurative or caseous, whereas the more chronic lesions were dry and brittle. Most NHPs, regardless of species, also displayed pericardial effusion.

The most common finding in the tracheobronchial, mesenteric, mandibular, axillary, and inguinal lymph nodes of all three NHP species was enlargement with edema, hemorrhage, or congestion when excised. Caseous lymphadenitis was a feature observed only in the tracheobronchial (Fig. 5F) and mediastinal lymph nodes. Of the 16 animals examined, 9 NHP spleens displayed distinct, 4 mm in diameter, slightly raised necrotizing foci throughout the parenchyma and capsular surface (Fig. 5G). Splenomegaly also was observed in some animals.

Table 3
Most common macroscopic lesions observed in the AGMs, CMs and RMs following *F. tularensis* aerosol exposure.

Gross lesions	Animal ID																		
	African green monkeys ($n = 5$)						Cynomolgus macaques ($n = 6$)							Rhesus macaques ($n = 5$)					
	1	2	3	4	5	Total	1	2	3	4	5	6	Total	1	2	3	4	5	Total
Pneumonia (consolidation), abscesses, pyogranulomas	–	+	–	–	–	**1/5**	–	+	+/–	+	+	+	**5/6**	+	+	+	+	+	**5/5**
Pulmonary congestion, hemorrhage, edema	+/–	+	+	–	+	**4/5**	–	+	+	+	+	+	**5/6**	+/–	+/–	+	–	+	**4/5**
Fibrinous/fibrous pleural adhesions (pleuritis)	–	+	+/–	–	+/–	**3/5**	–	+	–	+	+	+	**4/6**	+	+	+	+	+	**5/5**
Thoracic fluid	–	+	–	–	–	**1/5**	–	–	–	+	+	–	**2/6**	–	–	–	–	–	**0/5**
Pericardial fluid	–	+	+	–	+	**3/5**	–	–	+	+	–	+	**3/6**	–	–	+	–	+	**2/5**
Enlarged (a), Suppurative or caseous exudate (b), congestion and/or hemorrhage (c)																			
Med/TB	–	+ (a,c)	+ (c)	+ (b)	+ (c)	**4/5**	–	+ (a,b,c)	–	+ (a,b,c)	+ (a,c)	+ (a,c)	**4/6**	+ (a)	+ (a,b)	+ (a,b,c)	+ (a,b)	+ (a)	**5/5**
Mandibular	–	+ (a)	+ (c)	–	+ (c)	**3/5**	–	+ (a,c)	+(c)	–	–	–	**2/6**	–	–	–	–	–	**0/5**
Mesenteric	–	+ (a)	–	+ (a)	+ (c)	**3/5**	–	+ (a,c)	–	+ (a,c)	–	+ (c)	**3/6**	+ (a)	+ (a,c)	+(a,c)	+ (a,c)	+ (a)	**5/5**
Axillary	–	+(a,c)	+ (c)	–	+ (c)	**3/5**	–	+ (a,c)	+(c)	+ (c)	–	–	**3/6**	–	–	+(a)	–	–	**1/5**
Inguinal	–	+ (a,c)	+ (a,c)	–	+ (a,c)	**3/5**	–	+ (a,c)	+(c)	+ (c)	–	–	**3/6**	+(a,c)	+ (a,c)	+(a)	+ (a)	–	**4/5**
Splenic abscess/pyogranulomas +/– splenomegaly, hemorrhage, congestion	–	+	+	+	+	**4/5**	–	+	+	+	–	+	**4/6**	–	–	–	–	+	**1/5**
Pancreatic abscess/pyogranulomas (* indicates hemorrhage, congestion only)	–	–	–	–	–	**0/5**	–	+	–	–*	–	–*	**1/6**	–	–	–	–	–*	**0/5**
Hepatomegaly, minimal to mild	–	+	–	–	–	**1/5**	–	+	+	–	–	–	**2/6**	–	–	–	–	–	**0/5**
GI mucosal hemorrhage/congestion	–	+	+	–	+	**3/5**	–	–	+	–	–	+	**2/6**	+	–	–	–	–	**1/5**

+ or – indicated the presence or absence of the gross lesion.
+/– indicates the variable presence of the gross lesion.

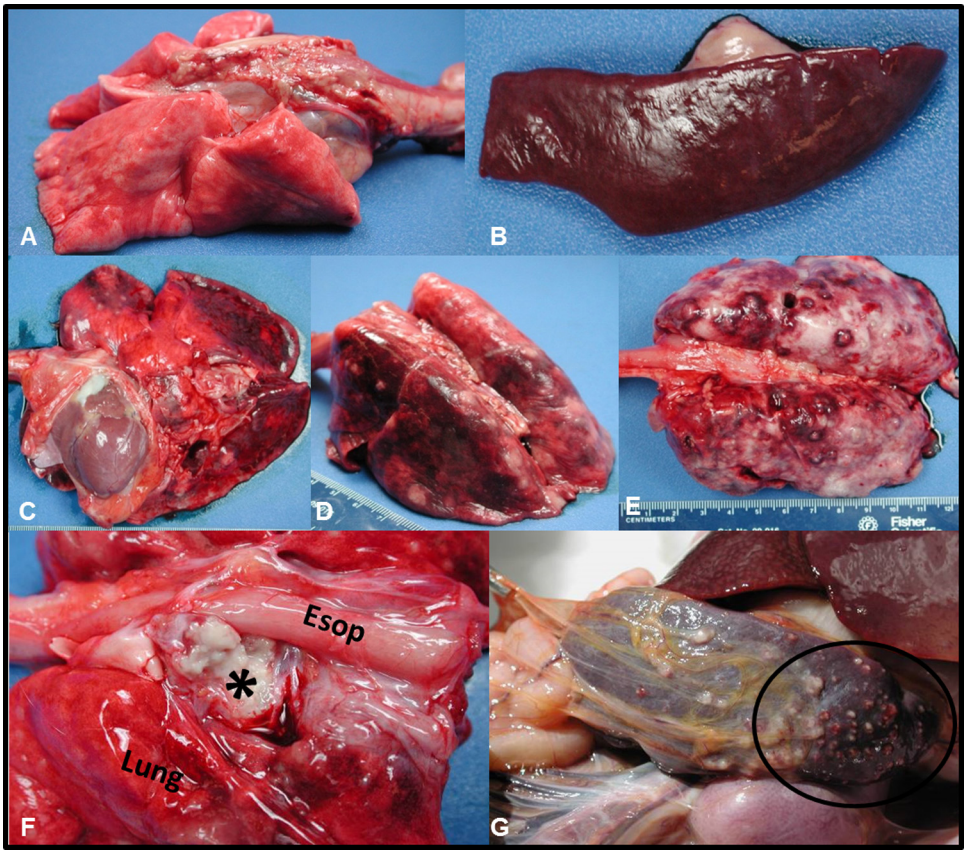

Fig. 5. Macroscopic findings in the lung, lymph node, and spleen of NHPs challenged by aerosol with *F. tularensis*. (A) Normal lung, non-challenged CM. (B) Normal spleen, non-challenged RM. (C) Lung, AGM 2 (D) Lung, CM 3, and (E) Lung, RM 2. Hemorrhagic, necrotizing, and/or pyogranulomatous foci on the pleural surface with congestion and edema and fibrinous pleuritis (most noticeable in the RM); note the failure of lung lobes to collapse. (F) Tracheobronchial lymph node, CM 2. The lymph node is effaced by tannish-white caseous material (*). (G) Spleen, CM2. A myriad of multifocal to coalescing, pale white, raised or flattened necrotic foci on the capsular surface. Esop = esophagus.

Some NHPs exhibited non-specific congestion and/or hemorrhage in the following tissues: pancreas, adrenal gland, liver, urinary bladder, reproductive organs, and gastrointestinal tract (Table 3).

3.7.2. *Histopathology*

Significant histopathologic changes were observed in 14 of the 16 animals studied. The surviving AGM and CM did not exhibit any pathological changes.

In those animals euthanized at day 10 or earlier, the most prominent finding was necrotizing and suppurative bronchopneumonia associated with larger conducting airways and arterioles (Fig. 6D). Extensive foci of hemorrhage, fibrin, edema, cellular and necrotic debris, and a mixed inflammatory infiltrate effaced both alveolar and bronchiolar architecture and partially occluded terminal bronchioles and alveoli. Fibrinous pleuritis also was common. Significant vascular necrosis with fibrin thrombi was observed in 3 of the 5 AGMs. By day 14, the hemorrhagic component was less prominent as the inflammatory component coalesced and formed vague or discrete chronic abscesses and pyogranulomas that elevated the pleural surface (Fig. 6E and F). Chronic abscesses were associated with extensive pleural thickening consisting of granulation tissue, fibrosis, and dilated lymphatic vessels. In less affected areas, an intra-alveolar mixed inflammatory infiltrate was apparent and edematous and congested alveolar septae were lined by alveolar epithelial cells (likely type II pneumocytes). Multinucleated giant cells were rare in all species. Multiple foci of necrotizing and ulcerative laryngitis and tracheitis were observed in some CM and RM subjects but not in any of the AGMs.

The lymph nodes, spleen, and bone marrow clearly were targets for aerosolized *F. tularensis* infection in the AGMs and CMs, and to a lesser extent in the RMs. The most consistent and severe histologic lesions, particularly in the AGMs and CMs, were observed in the mediastinal and tracheobronchial lymph nodes, and consisted of necrotizing to pyogranulomatous inflammation that effaced nodal architecture, which resulted in severe lymphoid loss (Fig. 6G). Additional lesions seen in some but not all lymph nodes included increased numbers of tingible body macrophages (TBMs) in the cortex, sinus histiocytosis and edema, draining hemorrhage, and erythrophagocytosis.

Similar to the lung lesions, the splenic lesions varied in histologic appearance from random foci of hemorrhage or severe lytic necrosis to well-demarcated, as large as 1 cm in diameter chronic abscesses and pyogranulomas (Fig. 6I).

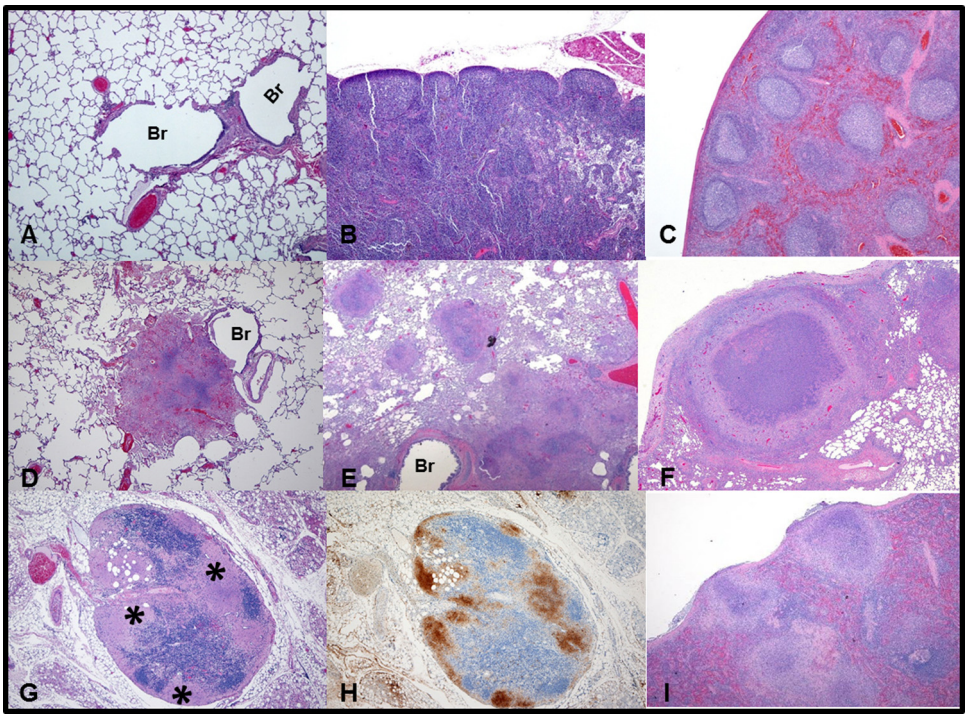

Fig. 6. Histopathological and immunohistochemical (IHC) analyses of lung, lymph node, and spleen of NHPs challenged by aerosol with *F. tularensis*. (A) Normal lung, non-challenged CM, HE 4×. (B) Normal tracheobronchial lymph node, non-challenged CM, HE 4×. (C) Normal spleen, non-challenged RM, HE 4×. (D) Lung, AGM 2, HE 4×; (E) Lung, CM 3, HE 2×; and (F) Lung, RM 2, HE 2×. Severe necrotizing to pyogranulomatous coalescing inflammatory foci, frequently associated with large airways and pulmonary vessels. (G, H) Tracheobronchial lymph node, AGM 3, HE 4× and *F. tularensis* IHC 4×. Severe lytic necrosis (*) effaces nodal architecture especially in the subcapsular and cortical areas; a serial section highlights strong bacterial antigen staining in the most severely affected areas. (I) Spleen, CM 2, HE 4×. Necrotizing and pyogranulomatous foci effaces splenic architecture and elevates the capsular surface. Br = bronchiole.

The larger lesions compressed the adjacent architecture and elevated and ruptured the splenic capsule. Additional splenic findings observed in some animals included hemorrhage and congestion, lymphoid depletion, and fibrosis (RMs only).

Multiple, often coalescing, necrotizing foci consistently were observed in the sternal bone marrow (necrotizing myelitis) of AGM and CM subjects, and less commonly in the RM. Generally, the marrow cavity was hypercellular with a noticeable increase in myeloid precursor cells, whereas mature neutrophils were observed infrequently.

Random necrotizing lesions confirmed by immunohistochemistry also were observed in various organs throughout the gastrointestinal, genitourinary, endocrine, cardiovascular, ophthalmic, and nervous systems in some animals.

3.7.3. *Immunohistochemical results*

In all NHP species, the strongest and most consistent *F. tularensis* immunoreactivity occurred in the lungs, followed by the spleen and tracheobronchial lymph nodes. Positive immunohistochemical staining was more widespread and affected more tissues in the AGMs and CMs than the RMs. Generally, immunolabeled intra- or extracellular bacteria, bacterial fragments, and/or antigen were present in areas where lesions were observed histologically, especially necrosis (Fig. 6H). Immunostaining enabled the detection of subtle lesions that might have been overlooked by routine light microscopy alone.

4. Discussion

Primary pulmonary tularemia is an important infectious disease to study because of its high lethality, confounding non-specific flu-like symptoms, and significant potential for both natural and artificial transmission. The development and licensure of tularemia medical countermeasures are dependent on compliance with the FDA's *Animal Rule*, which requires well-characterized animal models when human studies are not possible. The NHP is almost invariably the preferred animal model for infectious diseases, including tularemia. This study sought to identify the species that mimics pulmonary tularemia disease in humans most effectively.

All of the NHP species that were evaluated demonstrated susceptibility to aerosolized *F. tularensis* and development of rapidly progressing acute infection. The AGM and CM species developed lethal infection when challenged with aerosolized *F. tularensis* Schu S4 at doses above 20 CFU, whereas, the observed lethal dose in the RM species was greater than 276,667 CFU. Following low-dose exposure the RMs developed chronic pulmonary lesions; they were susceptible to disease but surprisingly resistant to its fatal effects.

Fever is one of the common clinical signs of pneumonic tularemia in humans and it ranges from 38 °C to 40 °C [11]. In this study, fever onset (defined as a 1.5 °C increase from baseline reading for 6 consecutive hours) was observed in all three species. Exposure to higher doses resulted in an onset of fever at 2 or 3 days PE in all three species. The AGM and CM exposed to high doses exhibited fever throughout the duration of the illness (i.e., animals were febrile until euthanasia criteria were met), with body temperatures often decreasing sharply in the hours before morbidity to the point of required euthanasia was reached. The range of fever in NHPs was 38–40.5 °C, similar to human disease.

Cytokine storm is a common mediator of immune responses against infectious agents. Cytokines are cell-secreted proteins that interact with other cells of the immune system to modulate bodily responses against disease and infection. Altered levels of certain plasma cytokines can indicate pathogenesis-associated inflammation, inform an intervention point, and/or predict imminent death. Proinflammatory cytokine IL-6, which is synthesized by macrophages and T-cells during fever and acute-phase response, increased sharply in all NHP species immediately before euthanasia criteria were met. G-CSF is produced by macrophages and endothelial cells in response to certain types of infections and conditions, and it stimulates the bone marrow to produce and release granulocytes. Most blood samples that were collected immediately prior to euthanasia exhibited increased G-CSF levels, possibly indicating the immune system's attempts to replenish the depleted granulocyte supply. Having observed associations between certain cytokine response patterns and imminent death, we believe the detection of certain cytokine patterns may serve as intervention and/or euthanasia criteria. However, studies with larger number of animals are needed to ascertain the statistical validity of these observations.

Individuals subjected to fatal or near-fatal aerosolized doses of infectious agents often develop bacteremia in the blood and/or tissues. The overall bacterial burden tended to be much lower in RM subjects relative to AGMs and CMs. All RM subjects, except for one, survived the experimental aerosol challenge. The longer survival times observed in these animals may explain the relatively low tissue burden but does not explain the low bacteremia results. As expected, the highest tissue bacterial burden was detected in the lungs. CMs consistently exhibited widespread dissemination with bacterial loads in all tissues tested.

Gross and histologic findings and immunohistochemical results are consistent with those previously described by Twenhafel et al. [12]. The obvious targets of *F. tularensis* following aerosol challenge of all three species included respiratory (e.g., lung, trachea, larynx) and hematopoietic (e.g., lymph nodes, spleen, bone marrow, tonsils) systems. However, macroscopic and histopathologic lesions varied in distribution and severity and often affected multiple body systems. As expected, pneumonic disease was the most common manifestation observed in all but the two animals challenged with the lowest doses of *F. tularensis*; the AGM (11 CFU) and CM (20 CFU) displayed no lesions 28 days after challenge.

Although necrotizing and hemorrhagic lesions were observed in multiple tissues of the animals that received the highest inhaled doses (except AGM 1 and CM 1), equally severe lesions often affecting a greater number of organs were observed in the AGM and CM subjects that had received considerably lower inhaled doses (40–801 CFU). Since all 3 of the highest dosed animals of each species succumbed to infection (i.e., met euthanasia criteria) by day 6, it is plausible that bacterial dissemination was stunted because the host died so soon. However, the three RMs that received 15,593 CFU, 11,211 CFU, or 2693 CFU survived the challenge, and upon necropsy, exhibited fewer changes in fewer target organs. Additionally, by day 8, histiocytic to pyogranulomatous inflammation was observed more readily in all animals although hemorrhage and necrosis remained typical histologic features, regardless of the inhaled dose.

In addition to the respiratory and hematopoietic lesions, random microscopic lesions were observed in various organs throughout the gastrointestinal, genitourinary, endocrine, cardiovascular, ophthalmic, and nervous systems in some but not all animals. Liver pathology similar to human disease was observed in all three NHP species following exposure to aerosolized *F. tularensis*. These pathologic findings, in addition to the bacterial load in the blood and tissues, indicate hematogeneous spread to other organs can cause a "typhoidal-like" disease syndrome in the NHP model following inhalation.

Of the three NHP species in this study, the RM was the most resistant to fatal outcomes of pulmonary tularemia, and its disease progression with chronic lesions is similar to human disease progression. Despite the advantages inherent to a model that mimics the human disease course, the RM model is problematic from the perspective of study planning since the signs of the disease are less clear and longer study periods are required to evaluate health, recovery, and survival. In addition, the lethal challenge doses for the RM are very high when compared to the infectious dose in humans.

Lethality was demonstrated in both the CMs and AGMs following exposure to relatively low doses of aerosolized *F. tularensis*, however, the CMs survived a few days longer at comparable doses. Disease progression of the CM also aligns with human disease progression, albeit not as well as the RM, but better than the AGM. Compared to the other 2 species, the CM most consistently manifested a clinical presentation of tularemia disease with fever, bacteremia, tissue bacterial burden, and clinical pathology, which are considered most heavily among various characteristics of an ideal laboratory-based model of human disease.

A major limitation of this study is the small number of subjects, which precludes strong statistical inference. However, this study provides a foundation for future research on medical countermeasures, enabling evidence-based development of protocols, dose schedules, animal model selection, and study length.

Conflict of interest

The authors declare no conflict of interest.

Disclaimer

Opinions, interpretations, conclusions, and recommendations are those of the authors and are not necessarily endorsed by the US Army or the Department of Defense.

Acknowledgements

We thank the personnel in the Aerosol Services Branch of the Center for Aerobiological Sciences for conducting the aerosol sprays of animals, the personnel of the Veterinary Medicine Division for the care and handling of the animals in these studies. Special thanks to Pathology Division's Dr. Nancy Twenhafel for pathology consultation; and Stephen Akers, Neil Davis, Gale Kreitz, and Chris Mech for providing necropsy, histochemical, and immunohistochemical support. Furthermore, we gratefully acknowledge Diana Fisher for her assistance with statistics. We also thank Dr. Kristin DeBord and Dr. Judy Hewitt (NIAID) for excellent discussion and guidance during this study and Dr. Tina Guina (NIAID) and Dr. Chris Whitehouse (USAMRIID) for critically reviewing the manuscript.

This study was supported by an interagency agreement between The Office of Biodefense Research Affairs (OBRA)/National Institute of Allergy and Infectious Diseases (NIAID) (now known as Office of Biodefense, Research Resources and Translational Research (OBRRTR) and USAMRIID.

References

[1] Carvalho CL, Lopes de Carvalho I, Ze-Ze L, Nuncio MS, Duarte EL. Tularaemia: a challenging zoonosis. Comp Immunol Microbiol Infect Dis 2014;37:85–96.
[2] Dennis DT, Inglesby TV, Henderson DA, Bartlett JG, Ascher MS, Eitzen E, et al. Tularemia as a biological weapon: medical and public health management. JAMA 2001;285:2763–73.
[3] Oyston PC, Sjostedt A, Titball RW. Tularaemia: bioterrorism defence renews interest in *Francisella tularensis*. Nat Rev Microbiol 2004;2:967–78.
[4] Croddy E, Krcalova S. Tularemia, biological warfare, and the battle for Stalingrad (1942–1943). Mil Med 2001;166:837–8.
[5] Christopher GW, Cieslak TJ, Pavlin JA, Eitzen Jr EM. Biological warfare. A historical perspective. JAMA 1997;278:412–7.
[6] Lyons RCW, Terry H. Animal models of *Francisella tularensis* infection. In: Abu Kwaik Y, Nano F, Sjostedt A, Titball R, editors. *Francisella tularensis*: biology, pathogenicity, epidemiology, and biodefense. New York, NY: The New York Academy of Sciences; 2007.
[7] Stundick MV, Albrecht MT, Houchens CR, Smith AP, Dreier TM, Larsen JC. Animal models for *Francisella tularensis* and *Burkholderia* species: scientific and regulatory gaps toward approval of antibiotics under the FDA Animal Rule. Vet Pathol 2013;50:877–92.
[8] Besch TK, Ruble DL, Gibbs PH, Pitt ML. Steady-state minute volume determination by body-only plethysmography in juvenile rhesus monkeys. Lab Anim Sci 1996;46:539–44.
[9] Hartings JM, Roy CJ. The automated bioaerosol exposure system: preclinical platform development and a respiratory dosimetry application with nonhuman primates. J Pharmacol Toxicol Methods 2004;49:39–55.
[10] Christensen DR, Hartman LJ, Loveless BM, Frye MS, Shipley MA, Bridge DL, et al. Detection of biological threat agents by real-time PCR: comparison of assay performance on the R.A.P.I.D., the LightCycler, and the Smart Cycler platforms. Clin Chem 2006;52:141–5.
[11] Matyas BT, Nieder HS, Telford III SR. Pneumonic tularemia on Martha's Vineyard: clinical, epidemiologic, and ecological characteristics. Ann N Y Acad Sci 2007;1105:351–77.
[12] Twenhafel NA, Alves DA, Purcell BK. Pathology of inhalational *Francisella tularensis* spp. tularensis SCHU S4 infection in African green monkeys (*Chlorocebus aethiops*). Vet Pathol 2009;46:698–706.